

**The Effect of Hydrostatic Pressure, Temperature and Impurity Position on the Binding Energy of a Hydrogenic Donor Impurity in a Quantum Dot.**

<sup>1</sup>OYENIYI Ezekiel and <sup>2</sup>POPOOLA Oyebola

<sup>1</sup>Applied Science Department,  
Kaduna Polytechnic, Kaduna State  
<sup>2</sup>Physics Department,  
University of Ibadan, Ibadan, Oyo state.

*Abstract*

---

---

*The effect of hydrostatic pressure, temperature, impurity position and radius of quantum dots on the binding energy of hydrogenic impurity was calculated using the variational method within the effective mass approximation. A spherical GaAs quantum dot surrounded by AlGaAs (with an infinite potential barrier) was considered. The results obtained show that; (a). Binding energy of the hydrogenic donor impurity increases with increase hydrostatic pressure and it is pronounced for narrower radii. (b) Binding energy of the hydrogenic donor impurity decreases with increase in temperature and this change is significant some particular change in temperature. (c) Binding energy of the hydrogenic donor impurity decreases with increase in impurity position. (d) Binding energy of the hydrogenic donor impurity decreases with increase in radius of the quantum dot.*

---

---

## 1.0 Introduction

Because of the recent advances in nanofabrication technology, it is possible to produce quantum dots whose characteristic dimensions are comparable with the electronic de Broglie wavelengths. The quantum mechanical nature of the electrons therefore plays a dominant role over the optoelectronic properties of the structure [1,2]. The presence of hydrogenic impurities is one of the main problems in semiconductor low-dimensional systems, since the presence of the impurity states in the nanostructure affects both the electronic mobility and the optical properties. Much work has been devoted to the study of hydrogenic impurity states in these systems. Binding energy calculations for hydrogenic impurities in quantum wells (QWs) [3, 4, 5], quantum well wires (QWWs) [3, 6, 7] and quantum dots (QDs) [8] have been performed.

The investigation of the electronic properties of hydrogen-like impurities in low-dimensional semiconductor heterostructures also attracts pretty much interest. It is explained by the vast possibility of purposeful manipulation of the impurity binding energy by means of external influences and, hence, the possibility of controlling the electronic and optical properties of functional devices based on such heterostructures [9]. The effects of external perturbation such as magnetic fields, hydrostatic pressure or electric fields on the physical properties of low-dimensional systems constitute a subject of considerable interest from both theoretical and technological points of view, due to the importance of these systems in the development of new semiconductor devices and applications. Recently, works on the effect of hydrostatic pressure temperature on binding energy of hydrogenic impurity in quantum wells and wires have been reported [10-12, 13] and to the best of our knowledge, very few have reported for quantum dot [14, 15]. Most of the works on quantum dot does not include the effect of temperature on binding energy of hydrogenic impurity.

In this work, using the variational procedure within the effective mass approximation, the binding energy of a hydrogenic impurity was investigated as functions of the sizes of the quantum dot, the applied hydrostatic pressure, temperature and the impurity position (on-and off-axis). Calculations are made in infinite potential barrier confinement.

---

---

Corresponding author: OYENIYI Ezekiel, E-mail: -, Tel.: +2348067086595

## 2.0 Theory

A spherical GaAs quantum dot surrounded by AlGaAs (with an infinite potential barrier) is considered. In the absence of an impurity, within the effective mass approximation, the Hamiltonian is given by

$$H_0 = -\frac{\hbar^2}{2m^*} \nabla^2 + V(r) \tag{2.1}$$

Where  $m^*$  is the effective mass of the electron. The confining potential  $V(r)$  is given by;

$$V(r) = \begin{cases} 0 & 0 \leq R \\ \infty & 0 > R \end{cases} \tag{2.2}$$

The eigenfunction for the lowest-lying state ( $n = 0, l = 0$ ) within the spherical dot of radius  $R$  is obtained using the ordinary Bessel function of order  $m = 0$  and is given by

$$\psi_0(r) = \begin{cases} N(\sin \alpha r)/r & 0 \leq R \\ 0 & 0 > R \end{cases} \tag{2.3}$$

Where  $N$  is the normalization constant. In order to satisfy the boundary condition  $\psi_0(r = R) = 0$ , the energies,  $E$  corresponding to equations 2.1 and 2.3 are

$$E_0 = \frac{\hbar^2 \alpha^2}{2m^*} \text{ and } \alpha = \frac{\pi}{R} \tag{2.4}$$

Under the influence of temperature and hydrostatic pressure, equation 2.4 becomes

$$E_0(P, T) = \frac{\hbar^2 \alpha^2}{2m^*(P, T)} \text{ and } \alpha = \frac{\pi}{R(P, T)} \tag{2.5}$$

$m^*(P)$  and  $R(P)$  are the effective mass electron and the radius of the spherical quantum dot as a function of hydrostatic pressure and temperature respectively.

The Hamiltonian for a hydrogenic impurity in spherical quantum dot of radius  $R$ , in the presence of hydrostatic pressure, can be given as

$$H = -\frac{\hbar^2}{2m^*(P, T)} \nabla^2 + V(r) - \frac{e^2}{\epsilon(P, T)|r - r_0|} \tag{2.6}$$

$\epsilon(P, T)$  is the dielectric constant as a function of pressure and temperature,  $e$  is the electronic charge.

$$|r - r_0| = \sqrt{r^2 + r_0^2 - 2rr_0 \cos \theta} \tag{2.7}$$

$r$  and  $r_0$  are the electron and impurity position respectively and  $\theta$  is angle between the electron and the impurity position.  $|r - r_0|$  is the electron-impurity distance.

The inclusion of hydrostatic pressure and temperature effects is made via the pressure temperature dependence on the electron effective mass, the GaAs static dielectric constant, and on the dimensions (radius). They are respectively given as [10, 13-14, 16, 17]

$$m^*(P, T) = \left[ 1 + \frac{15020 \text{meV}}{E_g(P, T)} + \frac{7510 \text{meV}}{E_g(P, T) + 341 \text{meV}} \right]^{-1} m_0 \tag{2.8}$$

$$\epsilon(P, T) = \begin{cases} 12.74 \exp(-1.73 \times 10^{-3} \text{kbar}^{-1} P) \times \exp[9.4 \times 10^{-5} \text{K}^{-1} (T - 75.6 \text{K})]; & T < 200 \text{K} \\ 13.18 \exp(-1.73 \times 10^{-3} \text{kbar}^{-1} P) \times \exp[9.4 \times 10^{-5} \text{K}^{-1} (T - 300 \text{K})]; & T \geq 200 \text{K} \end{cases} \tag{2.9}$$

$$R(P) = R(0)[1 - 2P(S_{11} + 2S_{12})]^{1/2} \tag{2.10}$$

Where  $m_0$  is the free electron mass,  $E_g(P, T)$  is the pressure and temperature dependent GaAs band gap,  $E_g(P, T) = 7510 \text{meV}$ . In the calculations, the values  $S_{11} = 1.16 \times 10^{-3} \text{kbar}^{-1}$  and  $S_{12} = -3.7 \times 10^{-4} \text{kbar}^{-1}$  are taken.  $R(P)$  is the radius of the sphere under the influence of pressure and  $R(0)$  is the radius of the sphere without the influence of pressure.

In order to get the impurity binding energy, we use a variational method and we consider the following trial wave function.

$$\psi = \psi_0 \exp(-\lambda|r - r_0|) \tag{2.11}$$

Where  $\lambda$  is the variational parameter and  $\psi_0(r)$  is the eigenfunction of the Hamiltonian in Eq. (1) without the impurity potential term.

Hence,

$$\psi(r) = \begin{cases} N(\sin \alpha r)/r \times \exp(-\lambda|r - r_0|) & 0 \leq R \\ 0 & 0 > R \end{cases} \tag{2.12}$$

The corresponding energy,  $E(P, T)$  is given as

$$E(P, T) = \min_{\lambda} \frac{\langle \psi | H | \psi \rangle}{\langle \psi | \psi \rangle} \tag{2.13}$$

The binding energy of a hydrogenic donor impurity,  $E_b$  is defined as the difference between the ground state energy of the system without impurity and the ground state energy of the system with impurity [12,18]; thus,

$$E_b(P, T) = E_0(P, T) - E(P, T) \tag{2.14}$$

### 3.0 Results and Discussions

In Fig4.1, for three different hydrostatic pressure values  $P = 0.0, P = 20.0\text{kbar}$  and  $P = 40.0\text{kbar}$  respectively, temperature,  $T = 4\text{K}$  and impurity position  $r^0/R = 0.0$ , the plot of binding energy of hydrogenic impurity as a function of radius of the quantum dot was obtained. It can be observed that binding energy of the hydrogenic impurity decreases with increase in the radius of quantum dot, for  $P=0.0$ . This is in agreement with the result reported in [14, 15]. Similarly, for other pressures ( $P = 20.0\text{kbar}$  and  $P = 40.0\text{kbar}$ ), the same results were obtained. Note that the binding energy increases with the hydrostatic pressure, reflecting the additional confinement due to the pressure; i.e. when the hydrostatic pressure is increased, the impurity and electrons becomes more confined. Also it can be observed that the pressure effect depends on quantum dot radius which is appreciable for narrow dots. The effect of hydrostatic pressure on the binding energy of the impurity reduces as the radius of the quantum dot increases much more.

Fig 4.2 shows the binding energy of hydrogenic impurity as a function radius of the quantum dot at three different impurity positions  $r^0/R = 0.0, r^0/R = 0.5, r^0/R = 0.9$  and at constant temperature and hydrostatic pressure ( $4\text{K}$  and  $40\text{kbar}$  respectively). It can be observed that binding energy decreases with increase in the radius. It can also be seen that binding energy decreases with increase in the impurity position in the quantum dot. This is in agreement with results in reported [15]. Furthermore, it can be observed that the curves begin to flatten out as the radius of dot increases and binding energy soon becomes a constant as the radius increased much more. In such a situation, significant confinement is no longer experienced. Considering  $r^0/R = 0.0$  and  $r^0/R = 0.5$ , the effect impurity position on the binding energy is significant for narrow dots as compared with wider dots. For impurity position close to the edge of the quantum dot, ( $r^0/R = 0.9$ ) relative to the origin ( $r^0/R = 0.0$ ) and ( $r^0/R = 0.5$ ), there is significant difference in the Binding energy at all points. Note that the effect of positions of impurity on binding energy decreases with radius.

Fig 4.3 shows the binding energy of hydrogenic impurity as a function impurity position for three different pressures ( $P = 0.0, P = 20.0\text{kbar}$  and  $P = 40.0\text{kbar}$ ) and at a radius  $R = 70.0\text{\AA}$  and temperature  $T = 4.0\text{K}$ . It can be observed that the binding energy of the hydrogenic impurity decreases with increase in impurity position but it (binding energy) increases with increase in hydrostatic pressure. This shows that hydrostatic pressure have effect on the confinement of the electron in the system depending on impurity position. The electronic confinement increases with hydrostatic pressure. This is in agreement with result reported in [15]. A minimum binding energy at impurity position close to the edge of the quantum dot can also be observed.

Fig 4.4 shows the binding Energy of the hydrogenic impurity as function impurity positions for three different radii ( $R = 70.0\text{\AA}, R = 140.0\text{\AA}, R = 210.0\text{\AA}$ ) and at constant temperature and pressure ( $4.0\text{K}$  and  $40.0\text{kbar}$  respectively). It can be observed that binding energy decreases with increase in the impurity position and also decreases with radius of the quantum dot. This is in agreement with results reported in [15]. Furthermore, it can be noted that the variation of binding energy with impurity position is more pronounced for smaller dots.

Fig4.5 shows the binding energy of the hydrogenic impurity as a function of pressure at impurity position ( $r^0/R = 0.0$ ) and  $T = 4.0\text{K}$ . It shows a linear dependence of binding energy on hydrostatic pressure. The binding energy of the hydrogenic impurity increases as the pressure increases. This is in agreement with results as found in [14, 19].

Fig4.6 shows binding energy of the hydrogenic impurity as a function of radius of quantum dot for three different temperatures,  $T = 4.0\text{K}, T = 196.0\text{K}$  and  $T = 300.0\text{K}$  at  $P = 40.0\text{kbar}$  and  $r^0/R = 0.0$ . It can be observed that binding energy decreases with increase radius of the quantum dot. This is in agreement with results in [11,20]. The effect of the change of temperature between  $4.0\text{K}$  and  $196.0\text{K}$  on binding energy is not significant as compared to the effect of the change of temperature between  $196.0\text{K}$  and  $300.0\text{K}$  on binding energy. Furthermore, it can also be observed that the temperature effect on the binding energy decreases with radius i.e there is reduction in electron confinement with increase in temperature.

In Fig 4.7, we have used quantum dot of radius  $R = 70.0\text{\AA}$ , pressure  $P = 40.0\text{kbar}$  in the plot of binding energy of hydrogenic impurity as function of impurity position for three different temperatures,  $T = 4.0\text{K}, T = 196.0\text{K}$  and  $T = 300.0\text{K}$ . It can be observed that the binding energy of the hydrogenic impurity decreases with increase in the impurity position. The effect of the temperature is such that, the binding energy of the hydrogenic impurity decreases with increase in temperature. This is in agreement with results in [20, 21]. Here, electronic confinement decreases with temperature. The effect of the change in temperature between  $T = 4.0\text{K}$  and  $T = 196.0\text{K}$  on electronic confinement in the system is small compare to change between  $T = 4.0\text{K}$  and  $T = 300.0\text{K}$  or  $T = 196.0\text{K}$  and  $T = 300.0\text{K}$ .

In Fig4.8, the parameters,  $R = 70.0\text{\AA}$ , pressure  $P = 40.0\text{kbar}$  and impurity position  $r^0/R = 0.0$  were used in the plot of

binding energy hydrogenic impurity against temperature. It shows a linear dependence of binding energy on temperature. The binding energy of the hydrogenic impurity decreases with increase in temperature though these changes are very low for temperature ranges  $T < 200.0K$ . An almost linear dependence of binding energy on temperature can be observed for ranges  $200.0K \leq T < 300.0K$ . The temperature effect on the binding energy will be pronounced when the first temperature is in the ranges of  $T < 200.0K$  (say  $T = 4.0K$ ), then the next in the range  $T \geq 200.0K$  (say  $T = 300.0K$ ).

**Table 4.1** Binding energy of hydrogenic impurity as a function quantum dot radius for three different hydrostatic pressures.

Radius of dot, ( $A^\circ$ )	Binding Energy of impurity ( $meV$ ) at $P = 0.0Kbar$	Binding Energy of impurity ( $meV$ ) at $P = 20.0Kbar$	Binding Energy of impurity ( $meV$ ) at $P = 40.0Kbar$
58.9834	166.9	171.20	175.80
78.6445	104.9	107.90	110.90
98.3056	74.23	76.40	78.67
117.9668	56.46	58.18	59.98
137.6279	45.09	46.51	47.99
157.2890	37.28	38.49	39.74
176.9502	31.64	32.68	33.78
196.6113	27.40	28.32	29.28
235.9335	24.10	24.93	25.79
255.5947	21.480	22.22	23.00

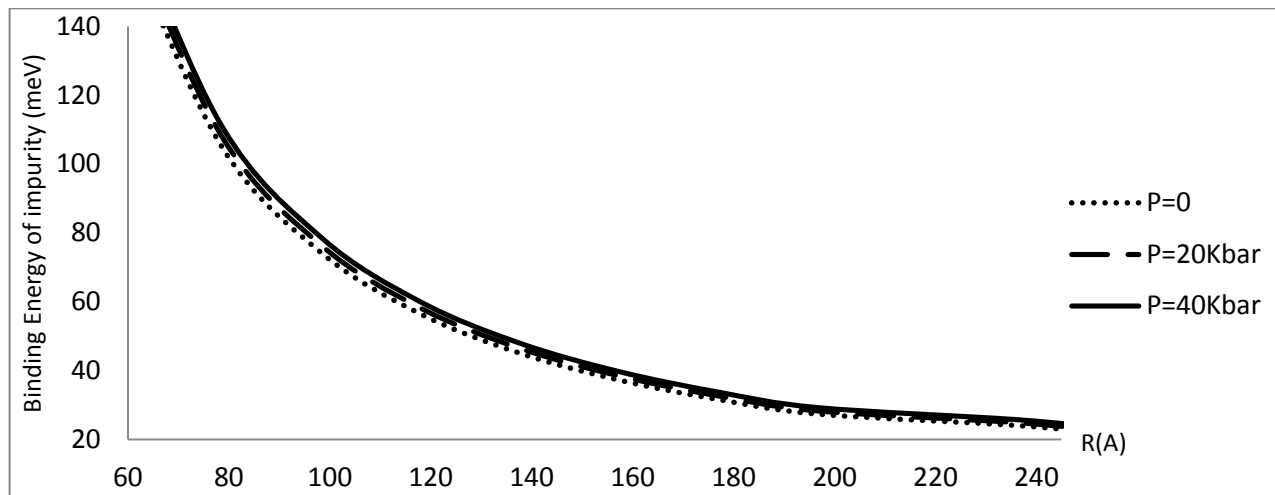


**Fig 4.1** Binding energy of hydrogenic impurity as a function quantum dot radius for three different hydrostatic pressures ( $P = 0.0, P = 20.0Kbar, P = 40.0Kbar$ ), impurity position,  $r_0/R = 0.0$  and temperature,  $T = 4.0K$ .

**Table 4.2** Binding energy of hydrogenic impurity as a function quantum dot radius for three different impurity positions.

Radius of dot, ( $A^\circ$ )	Binding Energy of impurity ( $meV$ ) at $r_0/R = 0.0$	Binding Energy of impurity ( $meV$ ) at $r_0/R = 0.5$	Binding Energy of impurity ( $meV$ ) at $r_0/R = 0.8$
58.9834	175.80	132.30	117.90
78.6445	110.90	82.28	74.31
98.3056	78.67	57.69	52.66
117.9668	59.98	43.56	40.13
137.6279	47.99	34.57	32.08
157.2890	39.74	28.44	26.55
176.9502	33.78	24.03	22.56
196.6113	29.28	20.72	19.54
216.2724	25.79	18.16	17.20
235.9335	23.00	16.13	15.34
255.5947	20.74	14.49	13.82

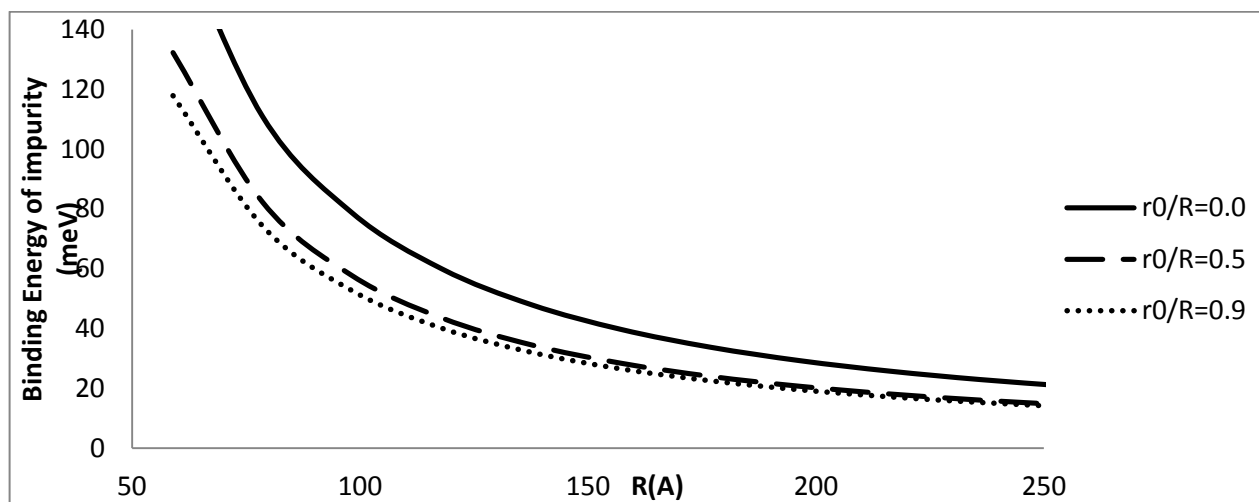


Fig4.2 Binding energy of hydrogenic impurity as a function quantum dot radius for three different impurity position ( $r_0/R = 0.0, r_0/R = 0.5, r_0/R = 0.9$ ) and temperature,  $T = 4K$ .

Table 4.3 Binding energy of hydrogenic impurity as a function impurity position,  $r_0/R$  for three different hydrostatic pressures.

Impurity position ( $r_0/R$ )	Binding Energy of impurity (meV) at $P = 0.0$	Binding Energy of impurity (meV) at $P = 20.0Kbar$	Binding Energy of impurity (meV) at $P = 40.0Kbar$
0.0000	129.80	133.30	137.00
0.1090	121.80	124.90	128.20
0.2180	112.30	115.10	118.10
0.3270	104.70	107.20	109.90
0.4360	98.57	100.90	103.40
0.5449	95.27	97.45	99.72
0.6539	89.80	92.02	94.32
0.7629	87.43	89.61	91.90
0.8719	86.68	89.01	91.47
0.9809	89.85	92.99	96.76

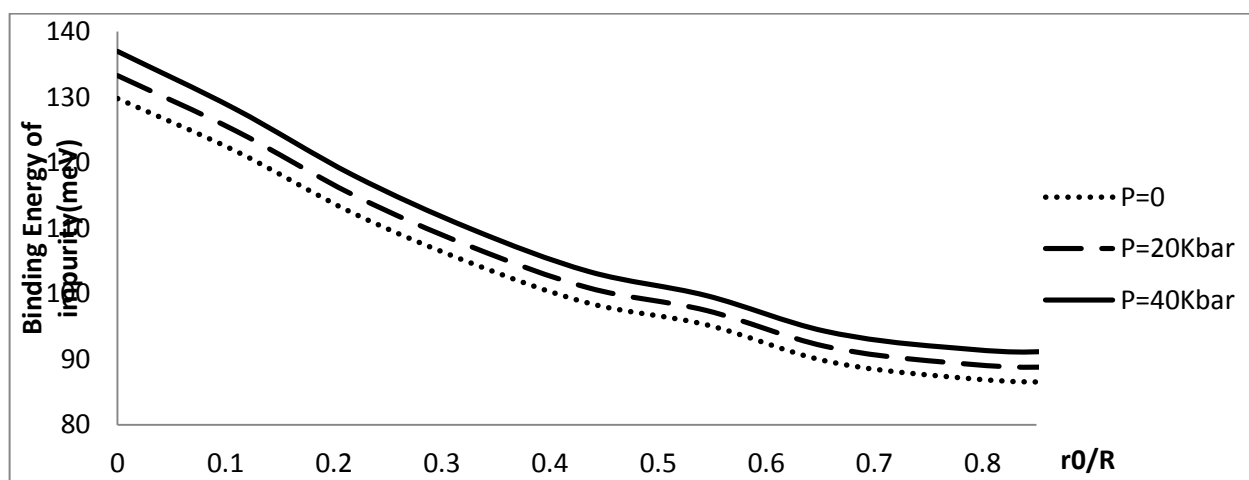


Fig4.3 Binding energy of hydrogenic impurity as a function impurity position,  $r_0/R$  for three different hydrostatic pressures ( $P = 0.0, P = 20.0Kbar, P = 40.0Kbar$ ), radius,  $R = 70\text{Å}$  and temp.,  $T = 4K$ .

Table 4.4 Binding energy of hydrogenic impurity as a function impurity position,  $r^0/R$  for three different radii.

Impurity position( $r^0/R$ )	Binding Energy of impurity (meV) at $R = 70.0A^0$	Binding Energy of impurity (meV) at $R = 140.0A^0$	Binding Energy of impurity (meV) at $R = 210.0A^0$
0.0000	137.00	47.99	27.43
0.1090	128.20	44.49	25.30
0.2180	118.10	40.50	22.88
0.3270	109.90	37.39	21.03
0.4360	103.40	35.03	19.65
0.5449	99.72	33.68	18.86
0.6539	94.32	32.02	17.98
0.7629	91.90	31.42	17.72
0.8719	91.47	31.74	18.04
0.9809	96.76	34.83	48.69

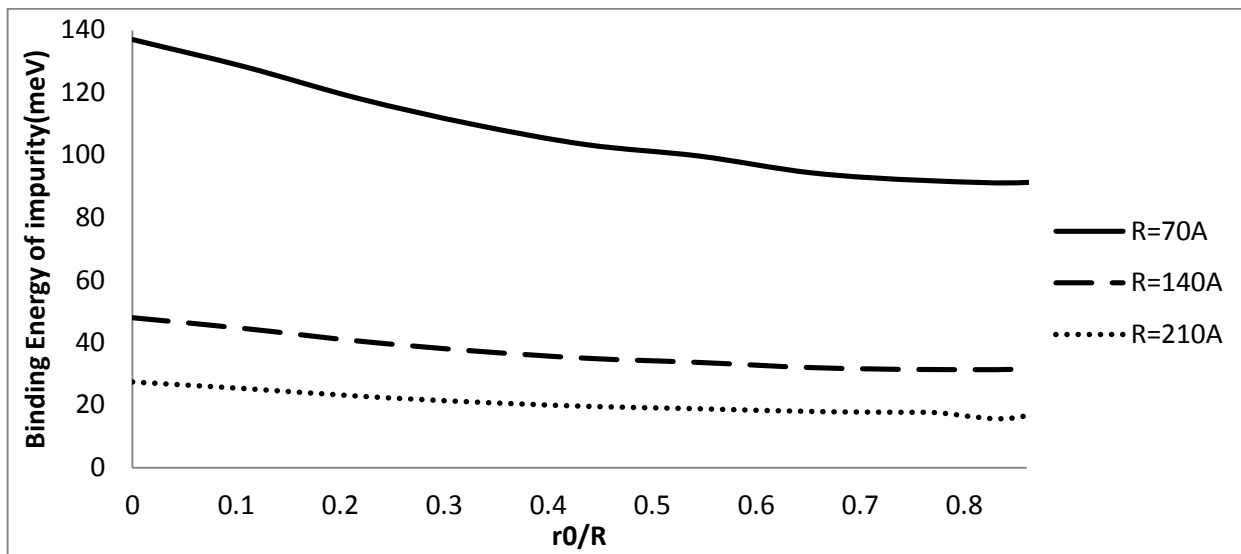


Fig4.4 Binding energy of hydrogenic impurity as a function impurity position,  $r^0/R$  for three different radii( $R = 70.0A^0$ ,  $R = 140.0A^0$ ,  $R = 210.0A^0$ ), pressure,  $P = 40.0Kbar$  and temp.,  $T = 4.0K$ .

Table 4.5 Binding energy of hydrogenic impurity as a function hydrostatic pressure at impurity position ( $r^0/R = 0.0$ ), radius,  $R = 70.0A^0$  and temperature,  $T = 4.0K$ .

Hydrostatic Pressure, $P(kbar)$	Binding Energy of impurity (meV)
0.00	129.80
10.00	131.60
20.00	133.30
30.00	135.20
40.00	137.00

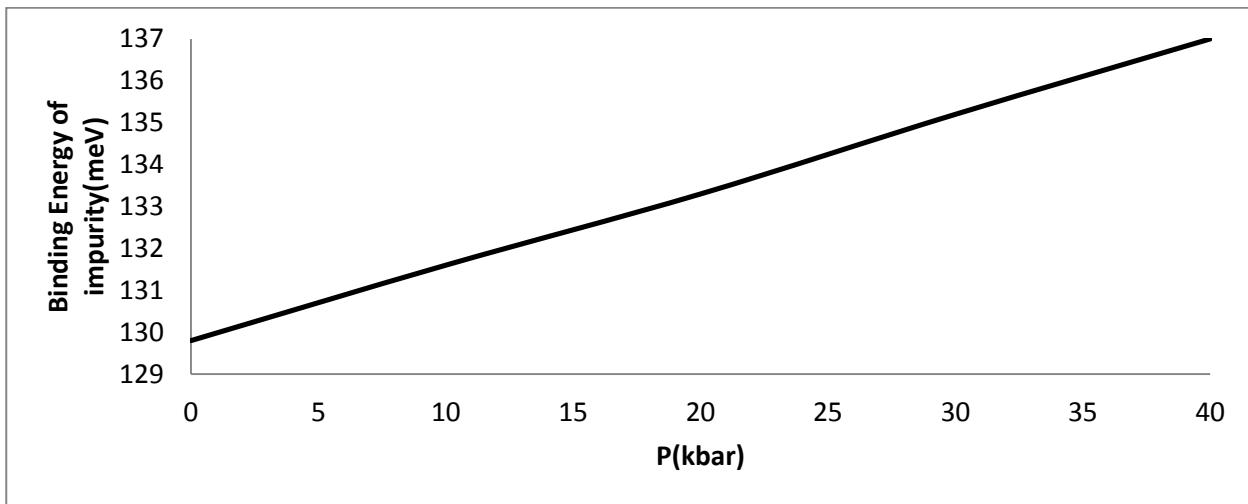


Fig4.5 Binding energy of hydrogenic impurity as a function hydrostatic pressure at impurity position ( $r_0/R = 0.0$ ), radius,  $R = 70.0A^0$  and temperature,  $T = 4.0K$ .

Table 4.6 Binding energy of hydrogenic impurity as a function quantum dot radius for three different temperatures.

Radius of dot, ( $A^0$ )	Binding Energy of impurity (meV) at $T = 4.0K$	Binding Energy of impurity (meV) at $T = 196.0K$	Binding Energy of impurity (meV) at $T = 300.0K$
58.9834	175.80	174.60	170.70
78.6445	110.90	110.00	107.10
98.3056	78.67	77.99	75.63
117.9668	59.98	59.40	57.44
137.6279	47.99	47.50	45.82
157.2890	39.74	39.31	37.85
176.9502	33.78	33.39	32.09
196.6113	29.28	28.94	27.76
216.2724	25.79	25.47	24.41
235.9335	23.00	22.72	21.74
255.5947	20.74	20.47	19.57

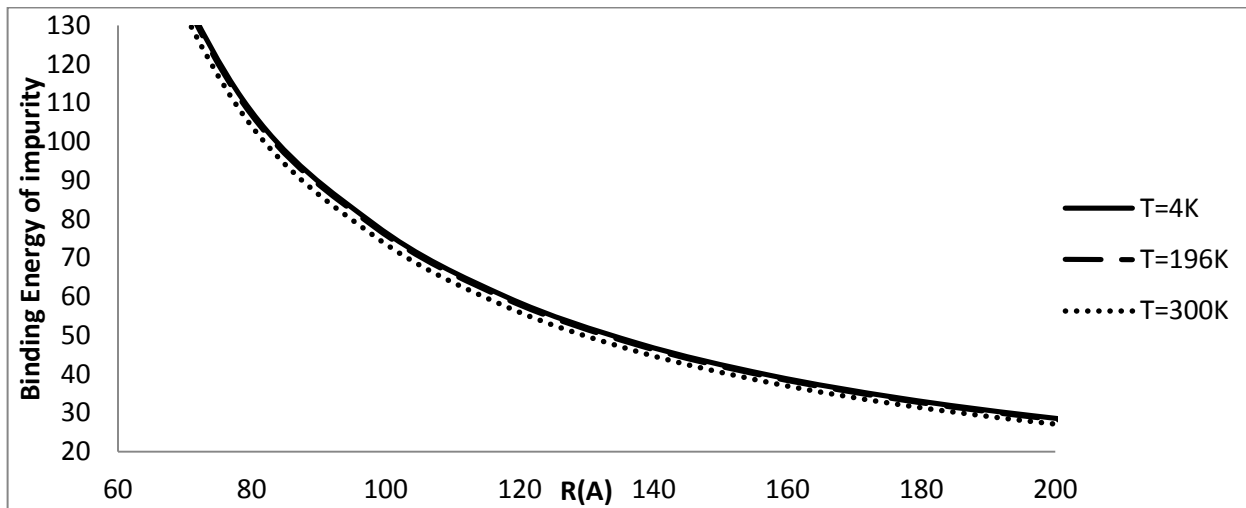


Fig4.6 Binding energy of hydrogenic impurity as a function quantum dot radius for three different temperatures ( $T = 4.0K, T = 196.0K, T = 300.0K$ ), and impurity position,  $r_0/R = 0.0$  and hydrostatic pressure,  $P = 40.0kbar$ .

Table 4.7 Binding energy of hydrogenic impurity as a function impurity position,  $r_0/R$  for three different temperatures.

Impurity position $r_0/R$	Binding Energy of impurity (meV) at $T = 4.0K$	Binding Energy of impurity (meV) at $T = 196.0K$	Binding Energy of impurity (meV) at $T = 300.0K$
0.0000	137.00	136.00	132.70
0.1090	128.20	127.30	124.30
0.2180	118.10	117.30	114.60
0.3270	109.90	109.10	106.70
0.4360	103.40	102.70	100.50
0.5449	99.72	99.09	96.95
0.6539	94.32	93.72	91.65
0.7629	91.90	91.30	89.23
0.8719	91.47	90.84	88.67
0.9809	96.76	95.99	93.35

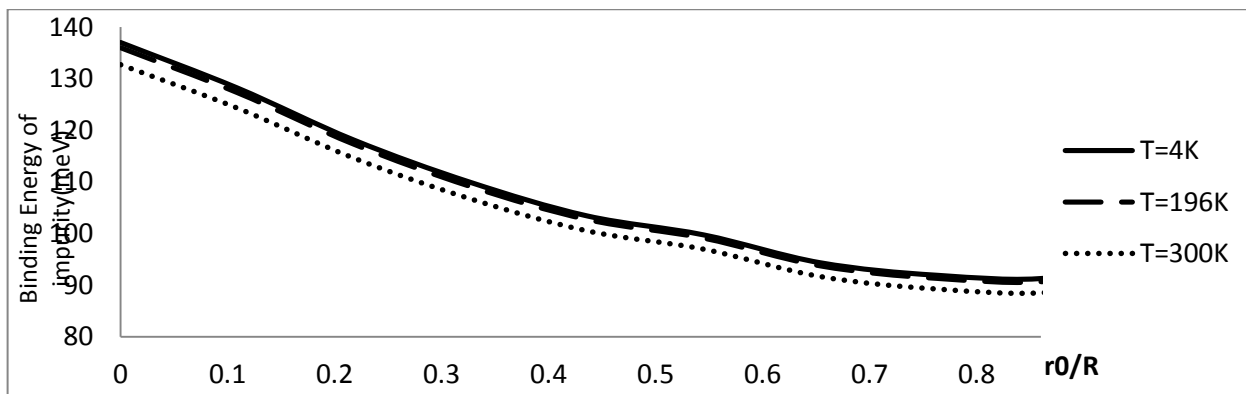


Fig4.7 Binding energy of hydrogenic impurity as a function impurity position,  $r_0/R$  for three different temperatures ( $T = 4.0K, T = 196.0K, T = 300.0K$ ), radius,  $R = 70.0A^0$  and hydrostatic pressure  $P = 40.0Kbar$ .

Table4.8 Binding energy of hydrogenic impurity as a function temperature at impurity positions ( $r_0/R = 0.0$ ), radius  $R = 70A^0$  and hydrostatic pressure,  $P = 40Kbar$ .

Temperature (K)	Energy of impurity (meV)
20.00	136.9
40.00	136.8
60.00	136.7
80.00	136.6
100.00	136.5
120.00	136.4
140.00	136.3
160.00	136.2
180.00	136.1
200.00	133.1
220.00	133.0
240.00	132.9
260.00	132.9
280.00	132.8
300.00	132.7



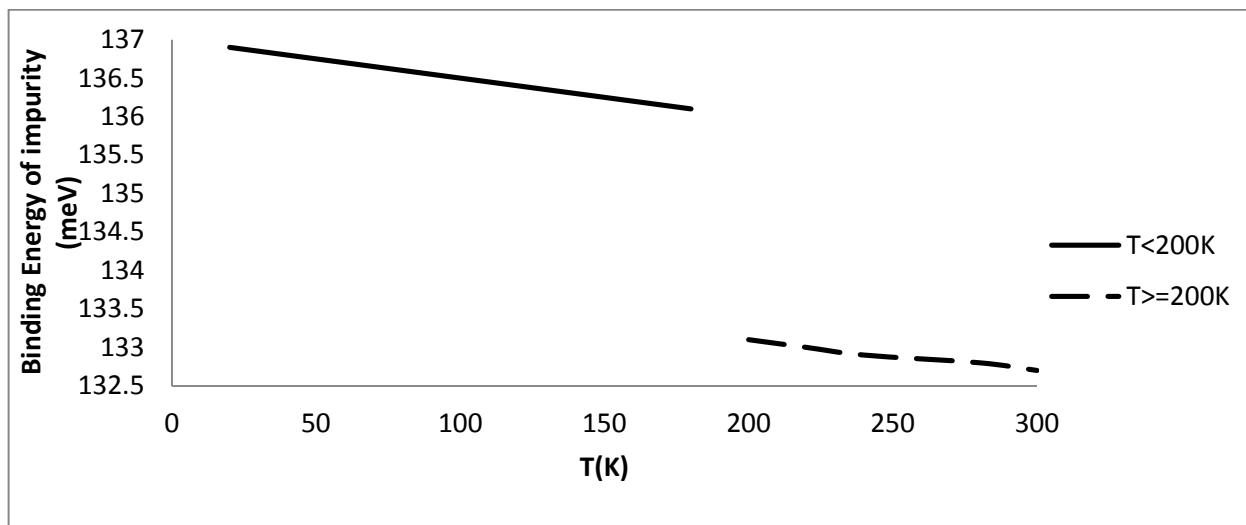


Fig 4.8 Binding energy of hydrogenic impurity as a function temperature at impurity position ( $r^0/R = 0.0$ ), radius,  $R = 70.0\text{\AA}$  and hydrostatic pressure,  $P = 40.0\text{kbar}$ .

## Conclusion

The effect of impurity position, hydrostatic pressure and temperature on the binding energy of impurity has been calculated. Binding energy of the hydrogenic impurity decreases with increase in impurity position from the origin toward the edge of the quantum dot. It was also observed that the binding energy decreases with increase in radius of the quantum dot i.e electronic confinement reduces with increase in radius and at much larger radius, very little or no confinement is experienced. Furthermore, binding energy of hydrogenic impurity increases with increase in hydrostatic pressure and this effect more pronounced for narrow dots. Lastly, it was observed that binding energy of hydrogenic impurity decreases with increase in temperature. The effect is well pronounced for a change in temperature from  $T < 200\text{K}$  (say  $T = 4\text{K}$ ) to  $T \geq 200\text{K}$  (say  $T = 300\text{K}$ ).

## References

- [1]. Bimberg D., (1999). Quantum dots: Paradigm changes in semiconductor physics. *Semiconductor* 33, 951 (1999) Volume 33, [Issue 9](#), pp 951-955
- [2]. Vivas-Moreno J. J. and Porrás-Montenegro N. (1998). The Effects of Quantum Confinement and Magnetic Fields on the Binding Energy of Hydrogenic Impurities in Low-Dimensional Systems. *Phys. Status Solidi* 210(6), 723.
- [3]. Brum J. A. (1985). Position-dependence of the impurity binding energy in quantum well wires *Solid State Commun.* 54, 179.
- [4]. Hassan H. H., El-Meshad N. (1997). Hydrogenic Impurity in Quantum Well Structures, 1p and 2s States Energy Calculations. *Phys. Stat. Sol. (b)* 201, 381.
- [5]. Weber G., (1995). Donors bound to X valleys in type-II GaAs–AlAs quantum well structures. *Appl. Phys. Lett.* 67, 1447.
- [6]. Brown J.W., Spector H. N., (1986). Impurity scattering limited momentum relaxation time in a quantum well wire. *J. Appl. Phys.* 59, 1179
- [7]. Bryant G.W., (1984). Hydrogenic impurity states in quantum-well wires *Phys. Rev. B* 29, 6632 (1984).
- [8]. Yoffe A. D., (1993). Low-dimensional systems: quantum size effects and electronic properties of semiconductor microcrystallites (zero-dimensional systems) and some quasi-two-dimensional systems. *Adv. Phys.* 42,173.
- [9]. Yoffe A. D. (2001). Semiconductor quantum dots and related systems: electronic, optical, luminescence and related properties of low dimensional systems. *Adv Phys.*50:1.
- [10]. Culchac F. J, Porrás-Montenegro N, Granada J. C., Latgé A. (2009). Hydrostatic pressure effects on electron states in GaAs-(Ga,Al)As double quantum rings. *J Appl Phys.*105:094324. doi: 10.1063/1.3124643.
- [11]. Emam, T. G. (2009). Effect of temperature on the binding energy of a shallow hydrogenic impurity in a quantum well wire. *Canadian Journal of Physics.* Vol. 87 Issue 11, p1159-1161.
- [12]. Eseau N., niculescu E. C. (2010). Hydrostatic Pressure And Temperature Effects On The Donor Binding Energy In Asymmetrical Square Quantum Wells. *U.P.B. Sci. Bull., Series A, Vol. 72, Iss. 1, 2010 ISSN 1223-7027*

- [13]. Manuk G. B., Ricardo L. R., Miguel E. M., Albert A. K., and Carlos A. D. (2012). Donor-impurity and related linear and non linear intraband optical absorption coefficients in quantum rings: effects of applied electric field and hydrostatic pressure. *Nanoscale Res Lett.* 2012; 7(1): 538 doi: [10.1186/1556-276X-7-538](https://doi.org/10.1186/1556-276X-7-538).
- [14]. Moscoso-Moreno C.A., Franco R., and Silva-Valencia J. (2007). The binding energy of light excitons in spherical quantum dots under hydrostatic pressure. *REVISTA MEXICANA DE FÍSICA* 53 (3) 189–193 JUNIO 2007.
- [15]. Perez-Merchancano S.T, Bolivar-Marinez L. E., Silva-Valencia J. (2007). Binding Energy of donor impurities in GaAs quantum dots under the effect of Pressure. *Revista Mexicana De fisica* 53(6) 470-474.
- [16]. Barseghyan M. G., Kirakosyan A. A., Duque C. A. (2009). Donor-impurity related binding energy and photoionization cross-section in quantum dots: electric and magnetic fields and hydrostatic pressure effects. *Eur Phys J B.* 72:521. doi: 10.1140/epjb/e2009-00391-0.
- [17]. Kopf R. F., Herman M. H., Lamont Schnoes M., Perley A. P., Livescu G., Ohring M., (1992). Band offset determination in analog graded parabolic and triangular quantum wells of GaAs/AlGaAs and GaInAs/AlInAs. *J. Appl. Phys.* 71, 1992, 5004.
- [18]. Baghramyan H. M., Barseghyan M. G., Duque C. A., and Kirakosyan A. A., (2013). Binding energy of hydrogenic donor impurity in GaAs/Ga<sub>1-x</sub>Al<sub>x</sub>As concentric double quantum rings: effects of geometry, hydrostatic pressure, temperature, and aluminum concentration. *Physica E*, vol. 48, no. 1, pp. 164–170.
- [19]. Alvarado-Reyes A.C., Silva-Valencia J., and Franco R. (2010). Effects of hydrostatic pressure and magnetic field on donor binding energies in an inverse parabolic quantum well. *Revista Mexicana de Física* 58 (2) 127–130.
- [20]. Bahramiyan H., Khordad R., (2013). Effect of various factors on binding energy of pyramid qdot: pressure, temperature and impurity position. (C) springer Science+ Business Media New York 3013. *Opt Quant Electron.* DOI 10.1007/s11082-013-9782-1.
- [21]. Sivakami A., Gavathri V. (2013). Hydrostatic pressure and temperature dependence of dielectric mismatch effect on the impurity binding energy in a spherical quantum dot. *Supperlattice and Microstructure*, ELSEVIER. Volume 58, pages 218-227.